Automated cropping intensity extraction from isolines of wavelet spectra

Bingwen Qiu
Fuzhou University, qiubingwen@fzu.edu.cn

Zhuangzhuang Wang
Fuzhou University

Zhenghong Tang
University of Nebraska - Lincoln, ztang2@unl.edu

Chongcheng Chen
Fuzhou University

Zhanling Fan
Fuzhou University

See next page for additional authors

Authors
Bingwen Qiu, Zhuangzhuang Wang, Zhenghong Tang, Chongcheng Chen, Zhanling Fan, and Weijiao Li

Published in *Computers and Electronics in Agriculture* 125 (2016), 11 pp. doi 10.1016/j.compag.2016.04.015

Submitted 17 March 2015; revised 8 April 2016; accepted 20 April 2016; published online 4 May 2016.

Automated cropping intensity extraction from isolines of wavelet spectra

Bingwen Qiu,[1] Zhuangzhuang Wang,[1] Zhenghong Tang,[2]
Chongcheng Chen,[1] Zhanling Fan,[1] and Weijiao Li[1]

1 National Engineering Research Centre of Geospatial Information Technology, Key Laboratory of Spatial Data Mining & Information Sharing of Ministry of Education, Fuzhou University, Fuzhou 350002, Fujian, China

2 Community and Regional Planning Program, University of Nebraska-Lincoln, Lincoln 68558, NE, USA

Corresponding author — B. Qiu, Spatial Information Research Centre of Fujian Province, Science Building, Floor 13th, Gongye Road 523, Fuzhou University, Fuzhou 350002, Fujian, China; email qiubingwen@fzu.edu.cn

Abstract

Timely and accurate monitoring of cropping intensity (CI) is essential to help us understand changes in food production. This paper aims to develop an automatic Cropping Intensity extraction method based on the Isolines of Wavelet Spectra (CIIWS) with consideration of intra-class variability. The CIIWS method involves the following procedures: (1) characterizing vegetation dynamics from time–frequency dimensions through a continuous wavelet transform performed on vegetation index temporal profiles; (2) deriving three main features, the skeleton width, maximum number of strong brightness centers and the intersection of their scale intervals, through computing a series of wavelet isolines from the wavelet spectra; and (3) developing an automatic cropping intensity classifier based on these three features. The proposed CIIWS method improves the understanding in the spectral–temporal properties of vegetation dynamic processes. To test its efficiency, the CIIWS method is applied to China's Henan province using 250 m 8 days composite Moderate Resolution Imaging Spectroradiometer (MODIS) Enhanced Vegetation Index (EVI) time series datasets. An overall accuracy of 88.9% is achieved when compared with in-situ observation data. The mapping result is also evaluated with 30 m Chinese Environmental Disaster Reduction Satellite (HJ-1)-derived data and an overall accuracy of 86.7% is obtained. At county level, the MODIS-derived sown areas and agricultural statistical data are well correlated ($r^2 = 0.85$). The merit and uniqueness of the CIIWS method is the ability to cope with the complex intra-class variability through continuous wavelet transform and efficient feature extraction based on wavelet isolines. As an objective and meaningful algorithm, it guarantees easy applications and greatly contributes to satellite observations of vegetation dynamics and food security efforts.

Keywords: Cropping intensity, Intra-class variability, MODIS EVI, Time-series, Wavelet isolines

1. Introduction

Increasing cropping intensity is an efficient and promising way to promote global crop production without converting more lands for agriculture (Atkinson et al., 2012). However, agricultural intensification (e.g., increasing cropping intensity) has associated environmental consequences such as degraded soil fertility, water pollution, reduced biodiversity, and changes in atmospheric constituents (Matson et al., 1997). The potential environmental and social impacts from higher cropping intensity need to be carefully evaluated (Atkinson et al., 2012; Ray and Foley, 2013). Timely availability of large-scale information on the cropping intensity is useful to manage agro-environmental ecosystems (Estel et al., 2016; Fana et al., 2014). Often cropping intensity information is only available as statistical data at the level of administrative units and does not have accurate spatial details (Gray et al., 2014; Qiu et al., 2014b). Therefore, reliable cropping intensity mapping is vital for improving agricultural decisions and guaranteeing environmental security (Fana et al., 2014; Gray et al., 2014).

Previous studies have been conducted for estimating cropping intensity based on remote sensing vegetation indices time series datasets (Biradar and Xiao, 2011; Estel et al., 2016; Galford et al., 2008; Lunetta et al., 2010; Zhang et al., 2008). Among them, the most frequently utilized method is calculating the peaks and troughs from the vegetation indices temporal profiles (Biradar and Xiao, 2011; Galford et al., 2008; Jain et al., 2013; Sakamoto et al., 2006, 2009). However, these methods are difficult to be engaged with uncertainties introduced by various situations such as data noise (Galford et al., 2008). Recent research efforts aim to improve included delineating rice cropping activities using wavelet transform and artificial neural networks (Chen et al., 2012a), a shape-matching cropping index mapping method (Liu et al., 2012), the k-means clustering method (Setiawan et al., 2014a) or iterative self-organizing data analysis technique algorithm (Nguyen et al., 2012) and setting constraint conditions affecting the peaks of vegetation indices temporal profiles (Chen et al., 2012b; Lv and Liu, 2010; Peng et al., 2011; Sakamoto et al., 2009).

There are at least two key challenges that needed to be further addressed. One challenge is introduced by intra-class variability of vegetation indices temporal profiles from croplands. The intraclass variability of the original MODIS vegetation index time series signals is almost inevitable due to complicated reasons such as altitudinal and latitudinal gradient, variations in climatic, local soil condition and land managements (Siebert and Ewert, 2012; Wardlow et al., 2007). Three typical groups of intra-class variability of original signals could generally be identified. The first group is the altered vegetation phenology shift (advancement or delay), reflected in a shifted vegetation indices temporal profile. It could be introduced by altitudinal and latitudinal gradient (Qiu et al., 2013b), inter-annual variability of climate conditions or any other possibilities (Böttcher et al., 2014; Cleland et al., 2007; Jeong et al., 2011). The second group is the varied plant growth, revealed by a strengthened (considerably better vegetation growth) or lessened vegetation indices temporal profile. It could be introduced by site-specific conditions such as fertility, water and management practices, and other potential reasons (Qiu et al., 2013a). The third group of intra-class variability is introduced by different vegetation types/agricultural crops (Davison et al., 2011). For example, the double-cropping croplands could be planted with two different combinations of agricultural crops (e.g., winter wheat plus maize, early rice plus late rice). Till now, the challenge of intra-class variability has not been efficiently accounted for yet (Foerster et al., 2012; Gumma et al., 2015; Liu et al., 2012; Yan and Roy, 2014).

Another challenge is the need for new perspective of developing automatic, accurate methods which are robust to inter-annual variability (Thenkabail and Wu, 2012). Automated and semiautomated classification methods of remote sensing imagery have been shown to both increase performance and efficiency, and thus, reduce workload (Ghamisi et al., 2014; Quin et al., 2014; Terletzky and Ramsey, 2014). However, most of the traditional methods rely heavily on ground-truth sites or human interpretation for developing standard vegetation indices profiles or establishing classification criteria. These approaches might be time-consuming, labor-intensive, and inconsistent across different regions and years (Terletzky and Ramsey, 2014; Thenkabail and Wu, 2012; Wu et al., 2014). Recently, the automatic approaches are favored in the field of croplands or forest disturbance mapping (Huang et al., 2010; Kennedy et al., 2007; Stueve et al., 2011; Thenkabail and Wu, 2012; Waldner et al., 2015; Wu et al., 2014; Yan and Roy, 2014). Significant efforts should be drawn in the field of automatic cropping intensity mapping (Chen et al., 2012a; Liu et al., 2012; Setiawan et al., 2014a).

In order to address these two significant challenges, this paper aims to develop an automatic Cropping Intensity extraction method based on the Isolines of Wavelet Spectra (CIIWS) obtained through continuous wavelet transform. The continuous wavelet transform has long been successfully applied for pattern recognition in agriculture and related research fields (Du et al., 2006; Gaucherel, 2002; Qiu et al., 2016, 2014a; Tseng et al., 2015; Zhang et al., 2014). These studies revealed that the wavelet spectra/ features could efficiently capture the major signals of our study objects (Zhang et al., 2014). The peak detection method based on continuous wavelet transform can identify both strong and weak peaks while keeping false positive rate low (Du et al., 2006). Therefore, the continuous wavelet transform is selected to detect the real peak pattern representing the vegetation growth cycles for mapping cropping intensity. In the following sections, we give a detailed description of our methodology and present its application in Henan Province, China using the Moderate Resolution Imaging Spectroradiometer (MODIS) Enhanced Vegetation Index (EVI) time series datasets.

2. Study area

The study area is Henan Province (Figure 1) in China. Henan Province is chosen since it ranked first in food production in China over the past decade. It is approximately 520 km long and 572 km wide. Henan Province is located between latitudes 31°23′–36°22′N, longitudes 110°21′–116°39′E. It is typically characterized with a warm temperate climate. The altitudes increase from 22 m in the east plain to 2319 m in the west mountain (Figure 1). Almost one half (47.5%) of its areas are cultivated (Henan, 2010). There are overall double crops, principally winter wheat plus maize, cultivated in the east and southwest portion. Winter wheat is sown in October, tillers during November to December, and harvests in late May or early June (Figure 2). Maize is sown immediately after the harvesting of winter wheat, and harvests from late September to early October. Single crop, primary single rice, is primary cultivated in the south portion. Single rice is transplanted in May and harvest in September. Some vegetables are cultivated near cities, especially in the middle portion (near the Provincial capital, Zhengzhou city). The cropping calendars of major crops are provided (Figure 2) with reference to our field survey data and the agro-meteorological data obtained from the National Meteorological Information Centre of China. According to our field survey, the average parcel size of double crop in plain is usually larger than 500 m × 500 m. The average parcel size of croplands near mountains and hills could generally be less than 250 m × 250 m.

Due to the varieties of crops, altitudes and other site-specific conditions (i.e. land fertility), these three typical groups of intraclass variability of original signals introduced by different vegetation types/agricultural crops, altered vegetation phenology shift and the varied plant growth are very common in Henan province. Therefore, the Henan province provides good opportunity for us to develop an automatic method which is robust to inter-annual variability.

3. Data collection

3.1. MODIS EVI time series datasets

MODIS images offered a distinct opportunity for mapping agricultural changes for spatial and temporal density coverage from regional to global scales at no cost (Gumma et al., 2015). MODIS surface reflectance 8-day composite level 3 (L3) 250-m data from 2011 to 2013 were obtained. The level 3 products have been atmospherically and geometrically corrected. With red (R), near-infrared (NIR) and blue (B) bands, EVI was then calculated as $2.5 / (NIR - R)/(NIR + 6.0R - 7.5B + 1)$ (Huete et al., 2002).

3.2. Field survey datasets and agricultural census data

The field survey data were gathered in early August 2012, early February, Late April and late July 2013, middle January and August 2014, respectively. UniStrong MG858 hand-held GPS receivers with the accuracy of 1 m were utilized for ground survey in field sites. At each sampling sites, we recorded the cropping pattern (e.g., winter wheat plus maize) and their corresponding phonological stages, and measure the distribution areas. A total of 375 ground truth points were collected (see locations in (Figure 1). Among them, 213 survey sites were double

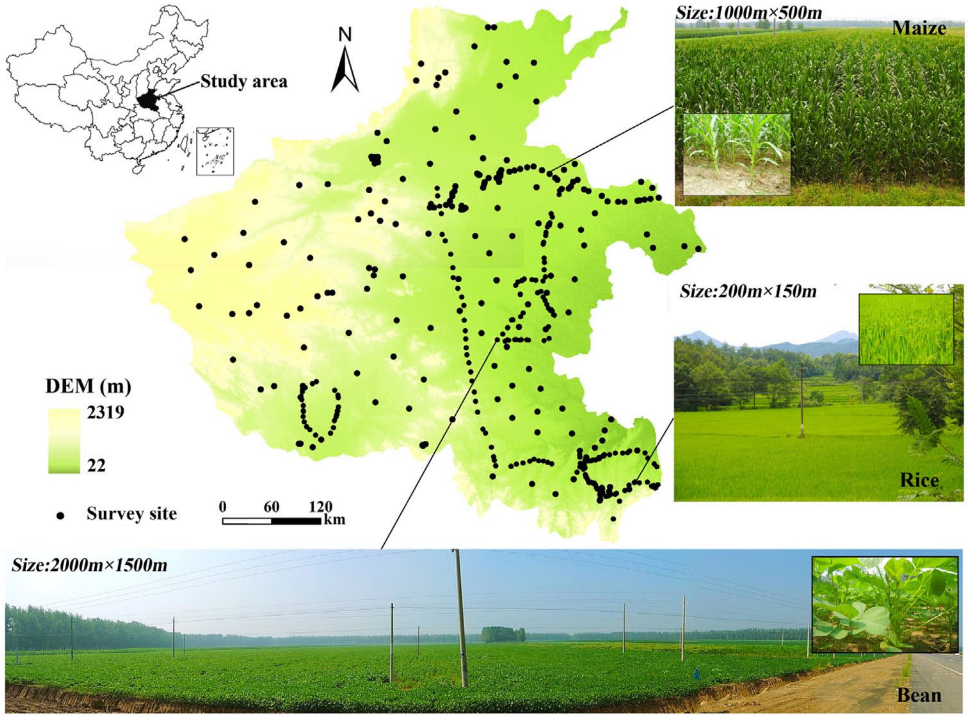

Figure 1. The study area and survey sites.

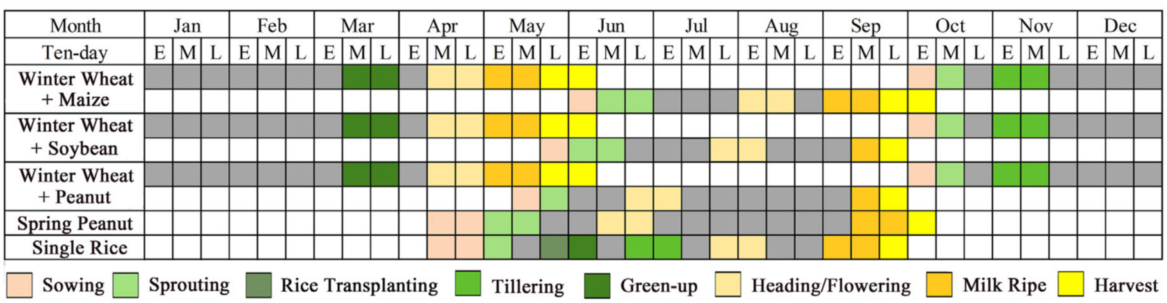

Figure 2. Cropping calendars of major crops in the study area.

crops, cultivated with winter wheat plus maize (190 sites), or winter wheat plus bean/peanut. Fifty-five survey sites were cultivated with single crop, primary single rice. These fields have a relatively long and stable planting history of at least 5 years and were distributed throughout the whole province. Other 95 survey sites were natural vegetation, primary the deciduous broadleaf forests.

In order to evaluate its accuracy, agricultural census data of sown areas at county level was downloaded from the Statistical Bureau of Henan province (NSHP) (http://www.ha.stats.gov.cn/hntj/index.htm).

3.3. Chinese Environmental Disaster Reduction Satellite images

In order to evaluate its accuracy with images with relatively higher spatial resolution, the Chinese Environmental Disaster Reduction Satellite (HJ-1 satellite for short) images are used. As part of the HJ satellite constellation, two optical satellites (HJ-1-A and HJ-1-B) are launched on September 6, 2008. The Charge Coupled Device (CCD) camera onboard can provide remote sensing data with four bands from visible to near infrared, with a spatial resolution of 30 m. HJ satellite data, operated by China Centre for Resources Satellite Data and Application, is freely available to the public. Detailed information could be found in English in recent crop classification studies applying HJ-1 images (Jia et al., 2013) and in Chinese at website http://www.cresda.com/n16/n1115/ n1432/index.html.

The cloud-free HJ-1 satellite images obtained from different dates (middle May, late July, middle October, middle December) are collected to identify cropping intensity. A total of twenty HJ-1 satellite images are applied. They are geometrically corrected and transformed to Universal Transverse Mercator projection. Images in autumn, winter, spring and summer are utilized to extract the distribution of natural vegetation (i.e., forests, grass), winter wheat, early crops and non-vegetation respectively. First, HJ-1 images in autumn are utilized to extract the distribution of natural vegetation (i.e., forests, grass); because no other live plants exist except natural vegetation (forests, grass) during that period (agricultural crops are already harvested in late autumn). Second, HJ-1 images in winter are applied to distinguish winter wheat. There are almost no live plants except winter wheat and evergreen forests in winter. Natural vegetation is already discriminated by images in late autumn. Additionally, winter wheat could easily be discriminated from the background since its spectral reflectance is distinctly different from that of the evergreen plants. Third, HJ-1 images in spring are utilized to extract the early crops. Finally, HJ-1 images in summer are adopted to distinguish non-vegetation. A threshold in the calculated Normalized Difference Vegetation Index (NDVI) is utilized to separate vegetated and non-vegetated areas. For a pixel, if there is classified winter wheat in winter or early rice in spring and also confirmed as vegetation in summer, it is identified as double-cropping croplands. Finally, if a pixel is not classified as non-vegetation, double-cropping cropland or natural vegetation, then it is assigned as single-cropping cropland. The cropping intensity distribution map in 2012 with a spatial resolution of 30 m is achieved. The cropping intensity distribution map interpreted from HJ-1 images is evaluated using the ground survey data. Over ninety percent (90.3%) survey points are correctly classified and indicates that the HJ-derived cropping intensity map could meet the requirements. The HJ-derived cropping intensity map is further resampled to 250 m target resolution by the majority resampling method, in order to be comparable with classification results from MODIS data.

4. Methods

Time series classification has been the subject of extensive research in the last several years (Douzal-Chouakria and Amblard, 2012). A first category of proposals consist of mapping a time series to a new description space where a conventional classifier could be applied (Douzal-Chouakria and Amblard, 2012). In this process, the original signals are transferred into the characteristic signals. Thus, the first category of proposals is termed the original-characteristic transferring process. A second category of works propose new heuristics, generally starting with the time series segmentation, to extract prototypes that best characterize the time series classes (Douzal-Chouakria and Amblard, 2012). During this process, those typical features/indicators are extracted from the characteristic signals which could be directly applied for classification or discrimination. The second category of works is termed as the feature selection and classification process. The proposed method for mapping cropping intensity based on isolines of wavelet spectra (CIIWS) combines these two categories of works: first, an efficient original-characteristic transferring process through continuous wavelet transform, and then a feature selection and classification process based on wavelet isolines. The CIIWS method comprises the following steps (Figure 3): data preprocessing, feature selection and crop intensity classifier. The entire procedure is executed using the Matlab software package (The MathWorks, Natick, Massachusetts, USA).

4.1. Data preprocessing

A daily continuous EVI time series is created using the date of observation following the procedure described in Qiu et al. study (2014a,b). First, non-vegetation areas are excluded by a simple threshold (Qiu et al., 2014b). Second, each observation (46 observations over the calendar year) with cloud contamination is discarded (94.18% pixels were cloud free observations). Third, the daily continuous EVI time series datasets are produced through linear interpolation during the study period of one year. Distinct EVI temporal profiles are observed in selected pixels of forest (111°4 4′17.804″E, 33°46′19.246″N) and single crop (115°12′36.198″E, 32°08′18.768″N) and double crops (114°35′12.148″E, 33°30′40.032 ″N), respectively (Figure 4). Compared with only one growth cycle observed from forest and single crop sites, the annual EVI profile from double crop site presents bimodal dynamics.

4.2. Original-characteristic transferring process through continuous wavelet transform

The continuous wavelet transform allows wavelet transforms at every scale with continuous translation. Mathematically, the continuous wavelet transform of a signal $f(t)$ is given as the below equation (Daubechies, 1990; Torrence and Compo, 1998).

$$W_\psi(a, b) = |a|^{½} \int_R f(t)\psi\left(\frac{t-b}{a}\right) dt \tag{1}$$

where $f(t)$ is the signal, a is the scale, b is the translation, $\psi(t)$ is the mother wavelet, $\psi_{a,b}(t)$ is the scaled and translated wavelet and W is the two-dimensional matrix of wavelet coefficients, called wavelet spectra. The wavelet spectra reflects the pattern matching between

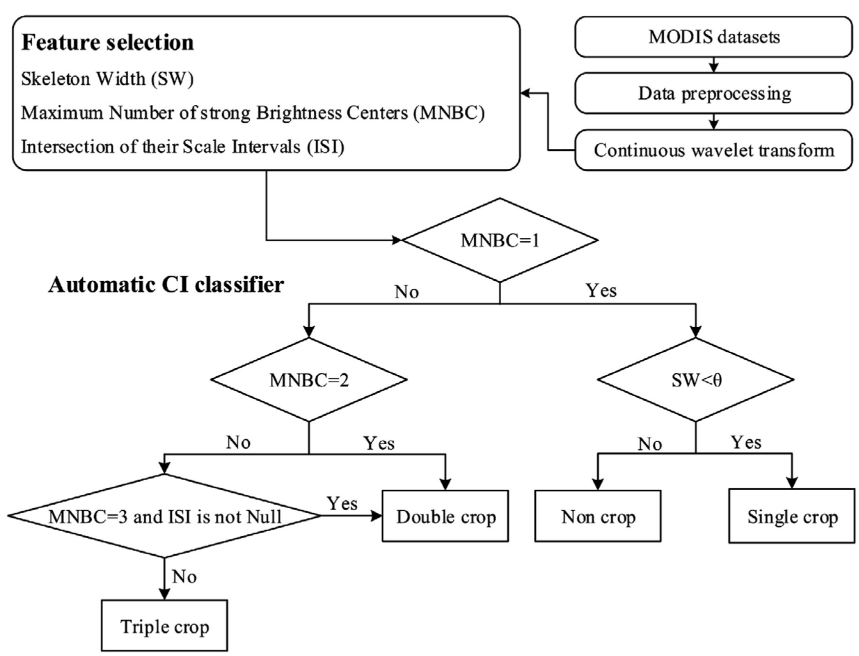

Figure 3. Overview of the methodology. Notes: Skeleton Width (SW), Maximum Number of strong Brightness Centers (MNBC) and the Intersection of their Scale Intervals (ISI).

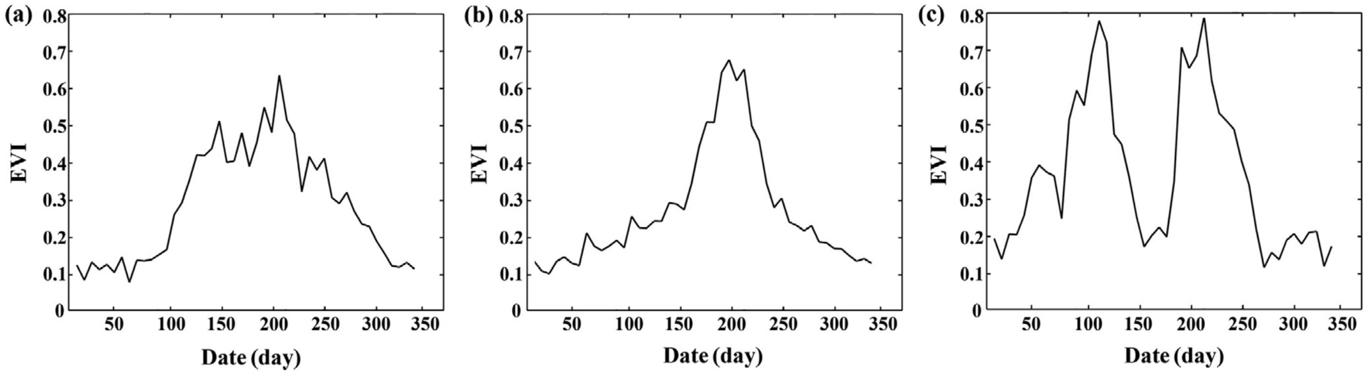

Figure 4. EVI temporal profiles of (a) forest, (b) single- and (c) double-cropping croplands.

the signal and mother wavelets at different scale and time. Strong values of wavelet coefficients denote better similarities between the signal and mother wavelets at that specific scale/time.

In order to get better performance of detecting growth cycle from vegetation index temporal profile, the wavelet should have the basic features of a peak. The Mexican hat wavelet is selected for this study, since it includes approximate symmetry and one major positive peak. Through continuous wavelet transform by the Mexican hat mother wavelet, the vegetation index temporal profiles are transformed into two-dimensional wavelet spectra (Qiu et al., 2014a, 2014b). Through continuous wavelet transform, distinct wavelet spectra are derived from the forest, single- and double-cropping croplands, respectively (Figure 5). It is obvious that there is at least one strong bright center with very strong wavelet coefficients observed from them. Strong bright centers represent the locations of best similarity between the vegetation index temporal profile and the mother wavelet. Here, it indicates the position of peak vegetation index values at specific scale/time, suggesting vegetation growth cycles.

4.3. Feature selection process

A feature selection process is conducted as follows. In step 1, the Skeleton Width (SW) is calculated based on the space between two skeleton lines (Figure 5). Wavelet isolines could be derived from the wavelet spectrum. There are numerous positive, negative and zero wavelet isolines observed at lower scales (high frequency). As the scale increases, only two zero wavelet isolines are generally examined. These two zero wavelet isolines, which extend from high to low scales, are termed the skeleton lines (Qiu et al., 2014b). The skeleton lines could be utilized as an indicator separating dense/sparse vegetated periods with relatively high/low EVI values (Qiu et al., 2014b). The space between these two skeletons lines at scale 1 is computed, which is termed as Skeleton Width (SW) (Figure 5).

In step 2, a series of positive wavelet isolines is achieved and tested for closeness. A series of positive wavelet isolines with wavelet coefficients from S to T (S is a positive value, $T > S$, T is the maximum of a wavelet spectrum. In this paper, S is 0.5, and T is 3) with step of 0.1 are computed within a certain scale range K (in this paper, the range from 0 to 160 is applied). These wavelet isolines with smaller values (i.e., 0.5) are relatively long and unclosed. As the values (wavelet coefficients) increase, these positive wavelet isolines gradually shrink inside and become close. The condition of closeness is evaluated for each positive wavelet isoline.

In step 3, the number of strong bright centers is calculated based on groups of these closed positive wavelet isolines. The close positive wavelet isolines obtained in step two are identified and sorted with their wavelet coefficients in ascending order. Two parameters, the maximum number of strong brightness centers (MNBC) and the maximum number of synchronously-obtained close positive wavelet isolines with one specific wavelet coefficients, are derived from the wavelet spectrum.

In step 4, if the maximum number of strong brightness centers equals to three, the Intersection of their Scale Intervals (ISI) is computed. Then it could be determined whether the intersection of their scale intervals is empty or not. This step is designed for the purpose of distinguishing the triple-cropping croplands.

4.4. Automatic cropping intensity classifier

The automatic cropping intensity classifier includes the following procedures (Figure 3). First, multiple-cropping croplands are identified based on the maximum number of strong brightness centers. For vegetation with a single growth cycle (i.e., a forest, natural grass and a single crop), the maximum number of strong brightness centers of its wavelet spectrum is a reflection of its growth cycle. Therefore, if the maximum number of strong brightness centers (MNBC) equals to 1, it is for single-cropping cropland or natural vegetation; otherwise it is for multiple-cropping croplands.

Second, single crop is distinguished from other vegetation types (natural vegetation) with reference to the Skeleton Width (SW). In temperate and subtropical regions, obvious seasonal cycles could be observed from EVI signals of vegetation: considerably higher in summer and lower in winter. These two skeleton lines could be applied as an indicator separating dense/sparse vegetated periods with relatively high/low EVI values (Qiu et al., 2014b). For vegetation with a single growth cycle, the skeleton width might reflect the relative length of the growing period. The growing lengths of single-cropping croplands are generally shorter than that of natural vegetation such as forests and grass. Therefore, the skeleton width is utilized as an indicator for separating single-cropping croplands and natural vegetation. The values of the skeleton width of natural vegetation and single-cropping croplands are both assumed to be normally distributed, which could be confirmed by evaluating the histogram across the whole study area. A simple threshold of skeleton width could be utilized for the purpose of classification.

Finally, double and triple crops are extracted based on both the maximum number of strong brightness centers (MNBC) and the Intersection of their Scale Intervals (ISI). Criteria quantification for double- and triple-cropping croplands is fairly complicated; information is further provided in the discussion section.

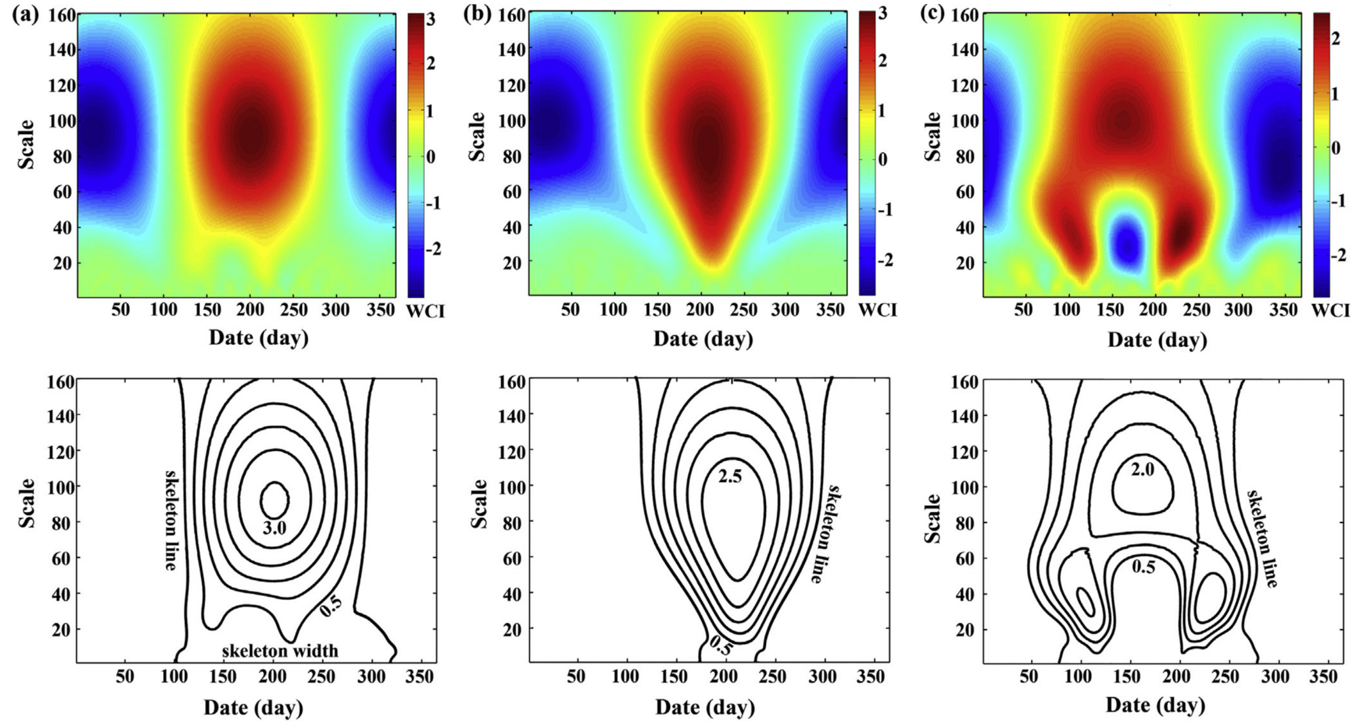

Figure 5. The wavelet spectra and its corresponding positive wavelet isolines of (a) forest, (b) single- and (c) double-cropping croplands. Notes: WCT: wavelet coefficients intensity.

4.5. Implementation and evaluation of the CIIWS

The entire procedure is executed using the Matlab software package (The MathWorks, Natick, Massachusetts, USA). The Matlab codes for deriving wavelet isolines of value z and evaluating its closeness are provided.

```
[Matrix_row,col] = contourf(W,[z,z]);
Rows = Matrix_row,col (1,:);
Cols = Matrixrow,col (2,:);
L = length(Rows);
Locations = find(Rows == z);
N = length(Locations);
K = 0;
For i = 1:N
    if i < N
        if Rows (Locations(i) + 1) == Rows (Locations(i + 1) _ 1) &&
    Cols (Locations(i) + 1) == Cols (Locations (i + 1) _ 1);
            k = k + 1;
        end
    elseif i == N
        if Rows (Locations(i) + 1) == Rows (L) && Cols (Locations (i)
    + 1) == Cols (L);
            k = k + 1;
        end
    end
end
```

In these codes, W is the wavelet spectra, z is the value of wavelet isolines, k records the number of closed wavelet isolines with value z. The function *contourf* (W, [z,z]) returns a two line matrix [$Matrix_{row,col}$], started with the flag "z" followed by the track of each wavelet isoline with value z. The row and column of the wavelet isoline with value z were saved in the first and second line in the matrix [$Matrix_{row,col}$], respectively. The function find(*Rows* == z) returns the location of its row of the flag "z". For one wavelet isolines, if the first row and column of its track in [$Matrix_{row,col}$] equals to last row and column of its track, it indicates that this specific wavelet isolines is closed.

For performance evaluation and validation of the CIIWS method, the ground truth observation data, agricultural census data and classification results from 30 m HJ-1 images are applied. Lastly, the overall accuracy, producer and user accuracy are calculated.

5. Results

5.1. Cropping intensity derived from MODIS through CIIWS method

A bi-modal distribution is observed in the histogram of the skeleton widths for all vegetation with single growth period in the study area (Figure 6). These two distributions of skeleton widths could be separated through the histogram minimums. Consequently, pixels with a skeleton width lower than the minimum 105 are classified as single-cropping croplands.

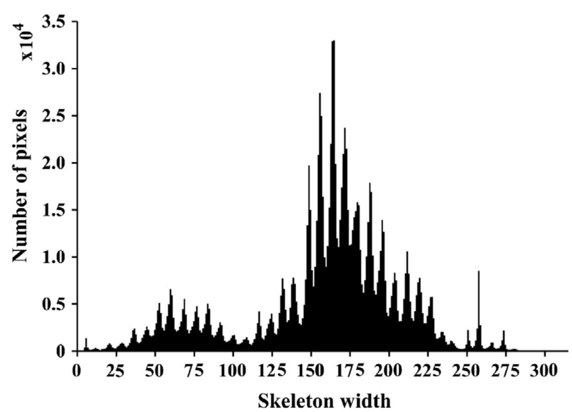

Figure 6. Histogram of skeleton width of vegetation with a single growth cycle.

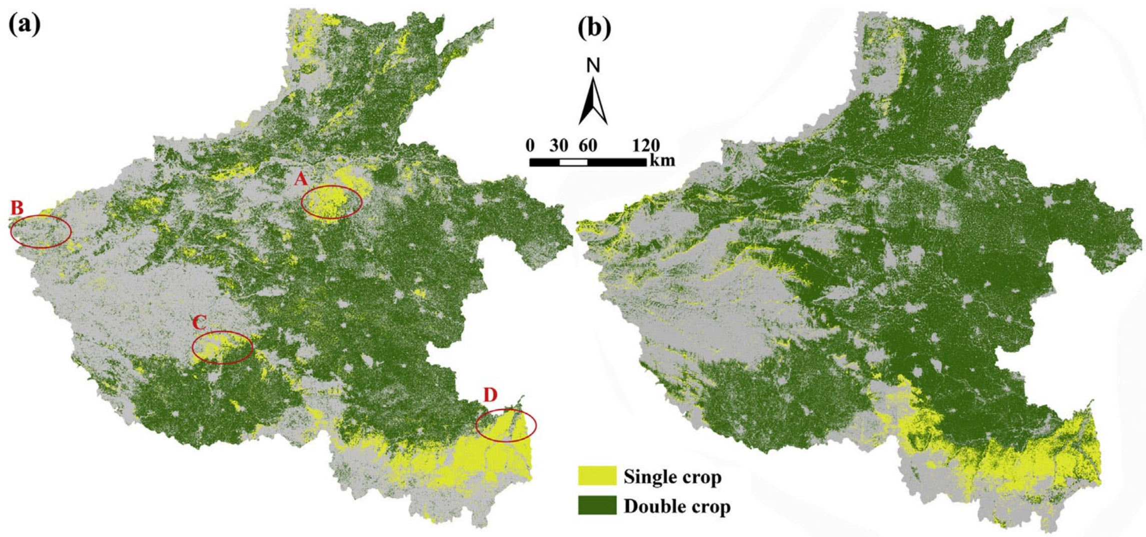

Figure 7. The crop intensity map in 2012 derived from (a) MODIS by CIIWS method compared with (b) HJ-1-derived data. Notes: Red circles A, B, C, D are four mismatched areas.

The spatial distribution of single- and double-cropping croplands in 2012 in Henan Province is given in Figure 7. With natural vegetation allocated in the west portion, the east and middle parts of Henan Province are primary double crops. The single- cropping crops are primarily cultivated in the southern portion.

5.2. Accuracy assessment

First, the accuracy assessment is conducted based on ground truth datasets collected at individual sites. The accuracies are 90.6% for double crops (193 out of 213), 85.5% for single crop (47 out of 55) and 87.4% for natural vegetation (83 out of 95). When compared with in-situ observation dataset, an overall accuracy of 88.9% is obtained.

Then, the CIIWS-generated sown area of agricultural crops is compared with that from the agricultural statistical database (http://www.ha.stats.gov.cn/hntj/index.htm). The sown area of cereals is calculated as the sum of twice the area of double-cropping croplands and the area of single-cropping croplands. These two datasets reach a good agreement, with an r-squared value of 0.85 (Figure 8, $N = 107$).

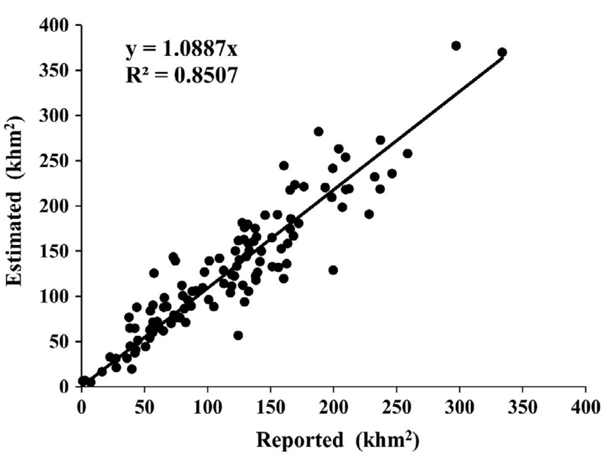

Figure 8. Correlation of sown land of agricultural crops between NSHP reports and MODIS-estimates at county levels.

Table 1. Accuracy assessment.

HJ-1 classification	MODIS classification: Single crop	Double crop	Others	Producer accuracy (%)
Single crop	113,263	8535	16,315	0.820
Double crop	74,042	1,090,175	149,234	0.830
Others*	40,901	67,235	1,125,722	0.912
User accuracy (%)	0.500	0.935	0.872	
Overall accuracy (%):	0.867			

* Others included natural vegetation and non-vegetation.

Finally, the similarity is analyzed between the spatial distribution maps derived from MODIS images through the CIIWS method and the HJ-1 derived images (Figure 7). The confusion matrix is calculated (Table 1). The producer accuracies of single and double-cropping croplands are 82.0% and 83.0% respectively. The total accuracy is 86.7%. The producer and user accuracies of single-cropping croplands are considerably lower due to misclassification between single crop and natural vegetation.

6. Discussion

6.1. The robustness to complex intra-class variability

For the purpose of efficient classification, the characteristic signals obtained through original-characteristic transferring process should not only diminish or even eliminate the intra-class variability, but also strengthen the signals. The original-characteristic transferring process applied in the CIIWS method through continuous wavelet transform is effective to the second group of intraclass variability described in the introduction section. To demonstrate this phenomenon, we strengthened or shifted the original MODIS EVI temporal signals deliberately and then compared their wavelet spectra obtained through continuous wavelet transform (Figure 9). The wavelet spectrum obtained from the strengthened signal (Figure 9b) conformed to that from the original signal (Figure 5c), revealing its robustness to the second group of intra-class variability (strengthened or lessened vegetation indices temporal profile). The wavelet spectrum obtained from the shifted signals

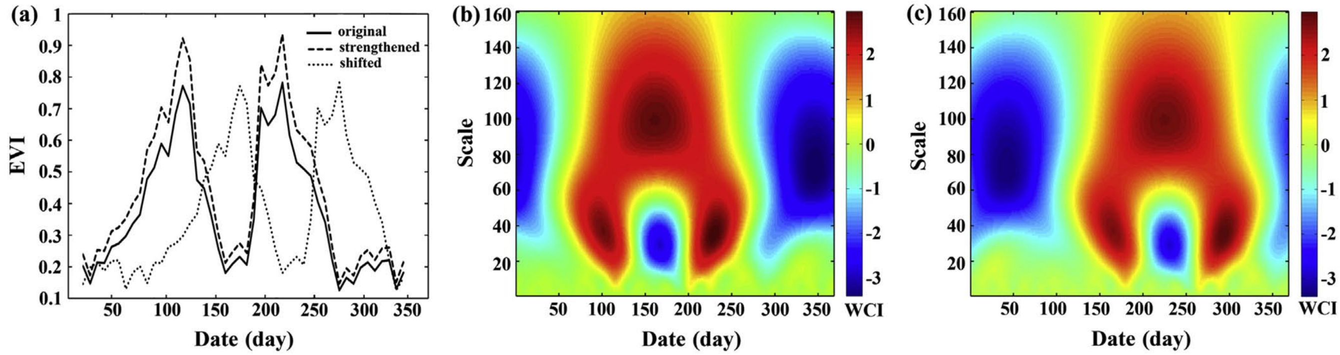

Figure 9. The original, strengthened, shifted MODIS EVI time series signal and its wavelet spectra. Notes: WCT: wavelet coefficients intensity.

also shifted (Figure 9c), revealing its sensibility to the first group of intra-class variability (shifted vegetation indices temporal profile). Additionally, the wavelet spectrum is also sensible to the third group of intra-class variability (different combinations of diverse crops or vegetation types).

Similarly, an excellent feature selection and classification process should be robust to intra-class variability but very sensible to inter-class variability. The feature selection and classification process of CIIWS method is robust to both the first and third groups of intra-class variability. The number of strong bright centers generally remained untouched with shifted vegetation phenology (Figure 9), suggesting its robustness to the first group of intraclass variability of vegetation indices temporal profile. As regards to its robustness to the third group of intra-class variability of vegetation indices temporal profile, it is explained as follows. For vegetation with single growth cycle, it is obvious that only one strong bright center is always obtained from their wavelet spectra. For double crops, the typical features (numbers of strong bright centers) obtained are fairly complicated, as introduced by the third group of intra-class variability. In general, the wavelet spectra of double-cropping croplands can be divided into two modes. The first mode is a roughly equal strong combination of two agricultural crop production cycles (Figure 5c). Its wavelet spectrum is characterized as with three obvious positive bright centers: (1) a dominant one at considerably lower frequency (around scale 100) representing the center of the relatively dense period separated by the two skeleton lines; and (2) another two at considerably higher frequency (around scale 30) denoting the center of those two agricultural cycles. The second mode is a combination of one relatively weak and one significantly strong agricultural cycle (Figure 10, pixel selected at 115°00′03.631″E, 34°20′47.209″N). Its wavelet spectrum is illustrated with one weak and one strong bright center: the weak one at considerably higher frequency (around scale 30) denoting the considerably weak agricultural cycle, and the strong one representing the relatively strong agricultural cycle (Figure 10). Only two strong bright centers are observed; the one at the relatively higher frequency is merged into the dominant one at lower frequency. From these above two modes of double crops, more than one strong bright center could always be obtained.

Through an efficient original-characteristic transferring, feature selection and classification process, the proposed CIIWS method are robust to those three typical groups of intra-class variability of vegetation indices temporal profiles. The proposed CIIWS method is capable of deriving cropping intensity efficiently and automatically. It does not require a large amount of input from field surveys or other training datasets. The criteria quantification process of the CIIWS method is objective and significant, compared with some other classifiers such as the nearest neighbor classifier or the artificial neural network (Chen et al., 2012a; Nguyen et al., 2012) which are unable to provide any form of explanation (Maletzke et al., 2014).

6.2. Comparison with the DCCWT and other methods

Qiu et al. (2014b) proposed a new methodology to map double-cropping croplands based on continuous wavelet transform (DCCWT). Similarly, the DCCWT method also attempted to deal with the intra-class variability of vegetation index temporal profile through continuous wavelet transform. Results obtained through DCCWT methods (Qiu et al., 2014b) are also visually conformed to HJ-1 image derived datasets (Figure 7b), revealing the efficiency of both methods in deriving CI. The biggest difference is located in these small patches in the middle and eastern portion of the study area. These small patches were identified as double-cropping croplands by the DCCWT method (Qiu et al., 2014b), but were correctly classified as natural vegetation by the CIIWS method which is confirmed by HJ-1 derived datasets (Figure 7b).

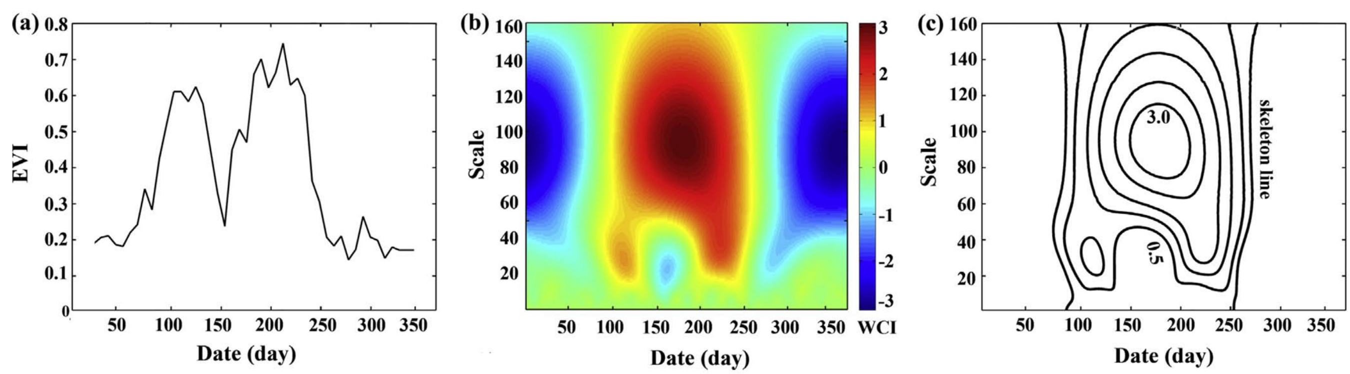

Figure 10. The EVI temporal profile, wavelet spectra and corresponding isolines of the second modes of double-cropping croplands.

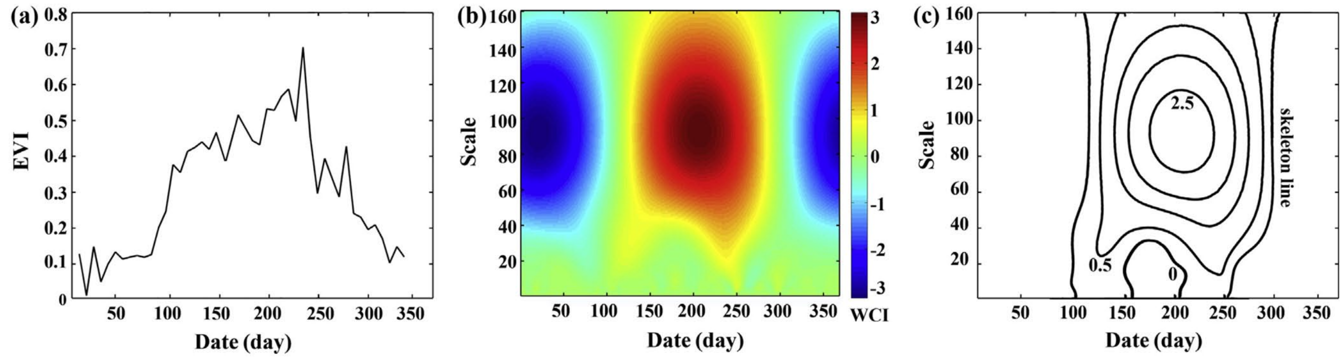

Figure 11. The EVI temporal profile, wavelet spectra and corresponding isolines of mismatched area with the DCCWT method.

The original MODIS EVI temporal profiles of these small patches in the middle and eastern portion are characterized as slightly reduced during their relatively higher EVI periods (Figure 11). Wavelet isolines with weak wavelet coefficients at relatively lower scales are easier to be introduced by slight fluctuations. Through deriving a feature selection process based on zero wavelet isolines, the feature peak obtained by the DCCWT method (Qiu et al., 2014b) might be very sensible to this kind of fluctuation, which might be caused by summer drought or other reasons.

Besides its relative higher accuracy compared with the DCCWT method (Qiu et al., 2014b), the CIIWS algorithm is also highly automatic and efficient. Instead of developing criteria based on the threshold of feature peak which relies on local distribution or ground survey data (Qiu et al., 2014b), the CIIWS algorithm proposes a meaningful cropping intensity classification standard which is robust to complex intra-class variability. Universal value could be utilized for this parameter required in the CIIWS method, guaranteeing great consistency and generality. This paper is expected to make significant contributions to global mapping efforts of land use intensity through developing an automatic cropping intensity mapping method (Kuemmerle et al., 2013).

6.3. Possible reasons for misclassifications

The MODIS-derived results estimated by CIIWS algorithm are consistent with in-situ observation data (over 85% agreement). When compared with the HJ-1 image derived distribution map, four mismatched areas (labeled as A, B, C, and D) are identified (Figure 7). There are at least two kinds of mismatch. The first kind of mismatch is due to vegetable cultivation. According to ground survey data and statistical datasets, area A is predominantly cultivated with vegetables (e.g., garlic, watermelon, or yam). Vegetable cultivation is generally different from other agricultural crops in the following two aspects. First, different vegetables might have very diverse growth cycles (very long or short). For example, some vegetables could be harvested within two months (leaf-eating vegetables), but some vegetables such as yam have more than a six month growing period (planted February, harvested in November, with a cropping index of 1). Therefore, vegetables might be harvested earlier or later than ordinary crops in autumn. Second, different vegetables would more likely be intercropped (e.g., garlic plus watermelon). Even if vegetables are not intercropped, an area of 250 m × 250 m would be easily planted with different species of vegetables with different harvesting dates. Consequently, crop shifting between different vegetables is less obvious than corn crop rotation. Therefore, vegetable cultivation could easily be misclassified as vegetation with single growth cycles. Area A is mainly identified as single crop or natural vegetation by the CIIWS method, since only one strong bright center could be obtained from its wavelet spectra of area A.

The second kind of mismatch might be the limitation of the 250 m resolution MODIS-based algorithm in identifying small patches of agricultural field sizes (Biradar and Xiao, 2011). Areas B, C, and D, located between plains and mountains or hills, are easily covered by a mixture of crops and natural vegetation (pictures in Figure 1, HJ-1 derived data in Figure 7). The mismatched sites with survey data are also generally located around the city (or town) surroundings or near mountains/hills, which posed more challenges in identification due to fragmentation and sub-pixel proportion of different vegetation/land cover classes (Pouliot et al., 2014; Qiu et al., 2014b; Setiawan et al., 2014b).

Until now, time series classification of vegetable cultivation is rarely reported and needed further investigations. Further field survey and investigation should be conducted to in order to define the complex intra-class variability of vegetable cultivation. Time series images with better spatial resolution should be utilized. The second kind of mismatching information could also be eliminated through applying the CIIWS method to higher spatial resolution images.

6.4. Future applications

The CIIWS method could also be applied in identifying triple-cropping croplands. Similar to double-cropping croplands, the wavelet spectra of triple crops could also be divided into two kinds of modes (Figure 12). The first mode is characterized with four obvious positive bright centers: one at relatively lower frequency (around scale 100) and the other three at considerably higher frequency (around scale 30), denoting the center of those three agricultural growth cycles. The second mode of triple crops is similar to the first mode of double crops, since both have three strong positive bright centers. However their relative locations of strong positive bright centers observed from these two modes are totally different. Criteria quantification of triple-cropping croplands is therefore provided as follows (Figure 3): if four groups of closed positive wavelet isolines are examined from their wavelet spectra, they are identified as triple-cropping croplands; if only three groups of closed positive wavelet isolines are observed and the intersection of the scale interval of these three derived wavelet isolines from each groups is empty, they are also classified as triple-cropping croplands.

The uniqueness of the CIIWS method is the ability to automatically compute cropping intensity across various regions on different years with time series images from diverse platforms. Besides the MODIS time series images, the proposed CIIWS method could also be applied to time series datasets of relatively higher-resolution images (e.g., Landsat TM, QuickBird, Rapid Eye and IKONOS). With easier accessibility and availability of remote sensing images, these time series classification methods hold great potential for various applications. The CIIWS method could easily be applied to other regions. Further investigations should be carried out to evaluate and determine the

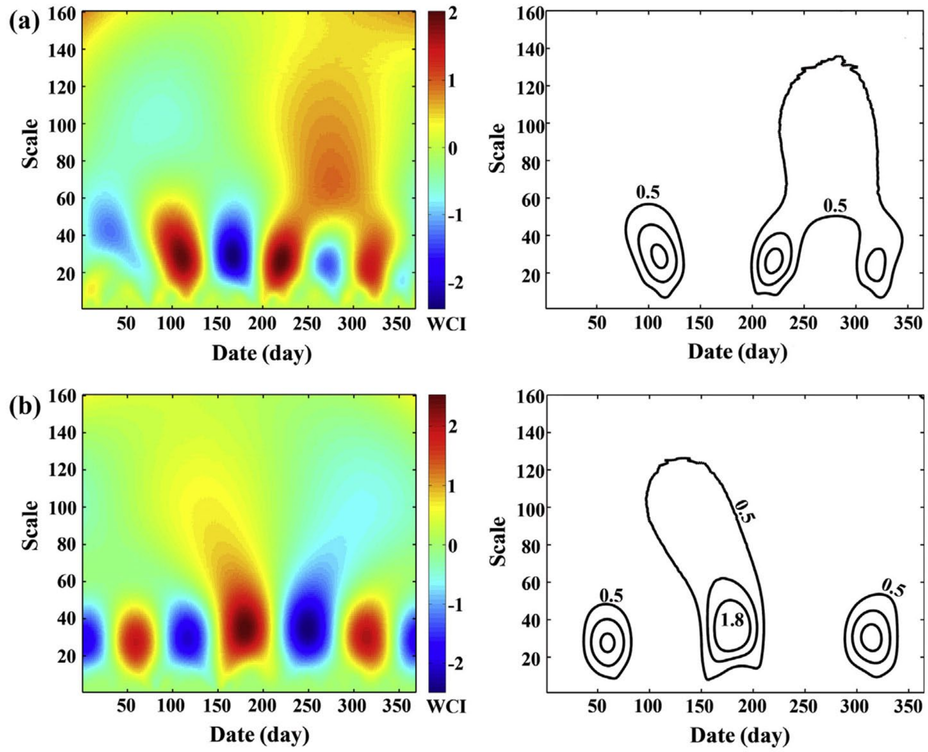

Figure 12. The wavelet scalogram and its corresponding isolines of the first (a) and the second (b) modes of triple-cropping croplands.

proper threshold from which to derive those positive wavelet isolines. There should always be a balance between classification accuracy and noise reduction. At relatively higher scales, wavelet isolines with much stronger wavelet coefficients are hardly sensible to noise. Therefore, the CIIWS method would be more robust for noise disturbance when the threshold of wavelet isolines increases. In that case, those identified multiple cropping croplands would be more typical, and the probability of misclassification of non-multiple crops or a mixture of multiple crops would be reduced. However, if the threshold is too large, the second mode of double-cropping croplands might not be correctly identified. On the other hand, if the threshold is relatively small, the mixed pixels and even totally non multiple crops could be classified as multiple crops. Particularly, if wavelet isolines are derived with a very small wavelet coefficient (e.g., 0.2), those wavelet isolines with very small wavelet coefficient are prone to noise disturbance at very small scales. Field surveys and other reference data could be applied to identify the proper threshold. Further investigations could be conducted in order to cope with this problem as regards to the relationships between the strength of wavelet coefficients and proportions of mixed pixels.

7. Conclusions

An innovative approach for accurately mapping cropping intensity is proposed in this paper. An automatic classification process is developed to smoothly derive indicators from isolines of wavelet spectra. The skeleton width and number of strong bright centers are applied as the primary metric to map cropping intensity. Its criteria quantification process is objective and meaningful. Its ability to compute cropping intensity automatically and accurately is verified through its applications in Henan province, China. This method is efficient in extracting cropping intensity through a robust feature selection process which could efficiently deal with complex intra-class variability. As an objective and automatic methodology, the CIIWS method could easily be utilized to other time series images of either coarse or high spatial resolution. Therefore, the CIIWS method has great potential of guaranteeing significant generality, comparability and consistency from local, regional to global scales. It is particularly suitable for developing countries, where rapidly changing ecosystems require updated information quickly. This paper is expected to make significant contribution to global, national and local earth observation efforts, such as the Group on Earth Observation Global Agricultural Monitoring (GEO GLAM) and National Agricultural Census of China.

Acknowledgments — The authors would like to thank NASA LP DAAC for making MODIS data publicly available online. This work is supported by the National Natural Science Foundation of China (Grant Nos. 41471362 and 41071267). We also appreciate the anonymous reviewers from Computers and Electronics in Agriculture for their constructive comments.

References

Atkinson, P.M., Jeganathan, C., Dash, J., Atzberger, C., 2012. Inter-comparison of four models for smoothing satellite sensor time-series data to estimate vegetation phenology. Remote Sens. Environ. 123, 400–417.

Böttcher, K., Aurela, M., Kervinen, M., Markkanen, T., Mattila, O.-P., Kolari, P., Metsämäki, S., Aalto, T., Arslan, A.N., Pulliainen, J., 2014. MODIS time-series-derived indicators for the beginning of the growing season in boreal coniferous forest- comparison with CO2 flux measurements and phenological observations in Finland. Remote Sens. Environ. 140, 625–638.

Biradar, C.M., Xiao, X., 2011. Quantifying the area and spatial distribution of double- and triple-cropping croplands in India with multi-temporal MODIS imagery in 2005. Int. J. Remote Sens. 32, 367–386.

Chen, C.F., Chen, C.R., Son, N.T., Chang, L.Y., 2012a. Delineating rice cropping activities from MODIS data using wavelet transform and artificial neural networks in the Lower Mekong countries. Agric. Ecosyst. Environ. 162, 127–137.

Chen, C.F., Son, N.T., Chang, L.Y., 2012b. Monitoring of rice cropping intensity in the upper Mekong Delta, Vietnam using time-series MODIS data. Adv. Space Res. 49, 292–301.

Cleland, E.E., Chuine, I., Menzel, A., Mooney, H.A., Schwartz, M.D., 2007. Shifting plant phenology in response to global change. Trends Ecol. Evol. 22, 357–365.

Daubechies, I., 1990. The wavelet transform, time–frequency localization and signal analysis. IEEE Trans. Inf. Theory 36, 961–1005.

Davison, J.E., Breshears, D.D., Van Leeuwen, W.J.D., Casady, G.M., 2011. Remotely sensed vegetation phenology and productivity along a climatic gradient: on the value of incorporating the dimension of woody plant cover. Glob. Ecol. Biogeogr. 20, 101–113.

Douzal-Chouakria, A., Amblard, C., 2012. Classification trees for time series. Pattern Recogn. 45, 1076–1091.

Du, P., Kibbe, W.A., Lin, S.M., 2006. Improved peak detection in mass spectrum by incorporating continuous wavelet transform-based pattern matching. Bioinformatics 22, 2059–2065.

Estel, S., Kuemmerle, T., Levers, C., Baumann, M., Hostert, P., 2016. Mapping cropland-use intensity across Europe using MODIS NDVI time series. Environ. Res. Lett. 11, 024015.

Fana, C., Zhenga, B., Myinta, S.W., Aggarwalb, R., 2014. Characterizing changes in cropping patterns using sequential Landsat imagery: an adaptive threshold approach and application to Phoenix, Arizona. Int. J. Remote Sens. 35, 7263– 7278.

Foerster, S., Kaden, K., Foerster, M., Itzerott, S., 2012. Crop type mapping using spectral–temporal profiles and phenological information. Comput. Electron. Agric. 89, 30–40.

Galford, G.L., Mustard, J.F., Melillo, J., Gendrin, A., Cerri, C.C., Cerri, C.E.P., 2008. Wavelet analysis of MODIS time series to detect expansion and intensification of row-crop agriculture in Brazil. Remote Sens. Environ. 112, 576–587.

Gaucherel, C., 2002. Use of wavelet transform for temporal characterisation of remote watersheds. J. Hydrol. 269, 101–121.

Ghamisi, P., Benediktsson, J.A., Sveinsson, J.R., 2014. Automatic spectral–spatial classification framework based on attribute profiles and supervised feature extraction. IEEE Trans. Geosci. Remote 52, 5771–5782.

Gray, J., Friedl, M., Frolking, S., Ramankutty, N., Nelson, A., Gumma, M., 2014. Mapping Asian cropping intensity with MODIS. IEEE J. Sel. Top. Appl. Earth Observ. Remote Sens. 7, 3373–3379.

Gumma, M.K., Mohanty, S., Nelson, A., Arnel, R., Mohammed, I.A., Das, S.R., 2015. Remote sensing based change analysis of rice environments in Odisha, India. J. Environ. Manage., 31–41

Henan, T.p.s.g.o., 2010. Henan Yearbook. The People Publisher of Fujian, Zhengzhou.

Huang, C., Goward, S.N., Masek, J.G., Thomas, N., Zhu, Z., Vogelmann, J.E., 2010. An automated approach for reconstructing recent forest disturbance history using dense Landsat time series stacks. Remote Sens. Environ. 114, 183–198.

Huete, A., Didan, K., Miura, T., Rodriguez, E.P., Gao, X., Ferreira, L.G., 2002. Overview of the radiometric and biophysical performance of the MODIS vegetation indices. Remote Sens. Environ. 83, 195–213.

Jain, M., Mondal, P., DeFries, R.S., Small, C., Galford, G.L., 2013. Mapping cropping intensity of smallholder farms: a comparison of methods using multiple sensors. Remote Sens. Environ. 134, 210–223.

Jeong, S.-J., Ho, C.-H., Gim, H.-J., Brown, M.E., 2011. Phenology shifts at start vs. end of growing season in temperate vegetation over the Northern Hemisphere for the period 1982–2008. Glob. Change Biol. 17, 2385–2399.

Jia, K., Wu, B., Li, Q., 2013. Crop classification using HJ satellite multispectral data in the North China Plain. J. Appl. Remote Sens. 7, 073576-073571-073512.

Kennedy, R.E., Cohen, W.B., Schroeder, T.A., 2007. Trajectory-based change detection for automated characterization of forest disturbance dynamics. Remote Sens. Environ. 110, 370–386.

Kuemmerle, T., Erb, K., Meyfroidt, P., Müller, D., Verburg, P.H., Estel, S., Haberl, H., Hostert, P., Jepsen, M.R., Kastner, T., Levers, C., Lindner, M., Plutzar, C., Verkerk, P.J., van der Zanden, E.H., Reenberg, A., 2013. Challenges and opportunities in mapping land use intensity globally. Curr. Opin. Environ. Sustain. 5, 484–493.

Liu, J.H., Zhu, W., Cui, X., 2012. A Shape-matching Cropping Index (CI) mapping method to determine agricultural cropland intensities in China using MODIS time-series data. Photogramm. Eng. Remote Sens. 78, 829–837.

Lunetta, R.S., Shao, Y., Ediriwickrema, J., Lyon, J.G., 2010. Monitoring agricultural cropping patterns across the Laurentian Great Lakes Basin using MODIS-NDVI data. Int. J. Appl. Earth Observ. Geoinf. 12, 81–88.

Lv, T., Liu, C., 2010. Study on extraction of crop information using time-series MODIS data in the Chao Phraya Basin of Thailand. Adv. Space Res. 45, 775–784.

Maletzke, A.G., Lee, H.D., Enrique, G., Batista, A.P.A., Coy, C.S.R., Fagundes, J.J., Chung, W.F., 2014. Time series classification with Motifs and characteristics. In: Espin, R., Pérez, R.B., Cobo, A., Marx, J., Valdés, A.R. (Eds.), Soft Computing for Business Intelligence. Springer, pp. 125–138.

Matson, P.A., Parton, W.J., Power, A., Swift, M., 1997. Agricultural intensification and ecosystem properties. Science 277, 504–509.

Nguyen, T.T.H., De Bie, C., Ali, A., Smaling, E.M.A., Chu, T.H., 2012. Mapping the irrigated rice cropping patterns of the Mekong delta, Vietnam, through hypertemporal SPOT NDVI image analysis. Int. J. Remote Sens. 33, 415–434.

Peng, D., Huete, A.R., Huang, J., Wang, F., Sun, H., 2011. Detection and estimation of mixed paddy rice cropping patterns with MODIS data. Int. J. Appl. Earth Observ. Geoinf. 13, 13–23.

Pouliot, D., Latifovic, R., Zabcic, N., Guindon, L., Olthof, I., 2014. Development and assessment of a 250 m spatial resolution MODIS annual land cover time series (2000–2011) for the forest region of Canada derived from change-based updating. Remote Sens. Environ. 140, 731–743.

Qiu, B., Feng, M., Tang, Z., 2016. A simple smoother based on continuous wavelet transform: comparative evaluation based on the fidelity, smoothness and efficiency in phenological estimation. Int. J. Appl. Earth Observ. Geoinf. 47, 91– 101.

Qiu, B.W., Fan, Z.L., Zhong, M., Tang, Z.H., Chen, C.C., 2014a. A new approach for crop identification with wavelet variance and JM distance. Environ. Monit. Assess. 186, 7929–7940.

Qiu, B.W., Zeng, C.Y., Tang, Z.H., Li, W.J., Hirsh, A., 2013a. Identifying scale-location specific control on vegetation distribution in mountain-hill region. J. Mt. Sci.- Engl. 10, 541–552.

Qiu, B.W., Zhong, M., Tang, Z.H., Chen, C.C., 2013b. Spatiotemporal variability of vegetation phenology with reference to altitude and climate in the subtropical mountain and hill region, China. Chin. Sci. Bull. 58, 2883–2892.

Qiu, B.W., Zhong, M., Tang, Z.H., Wang, C.Y., 2014b. A new methodology to map double-cropping croplands based on continuous wavelet transform. Int. J. Appl. Earth Observ. Geoinf. 26, 97–104.

Quin, G., Pinel-Puyssegur, B., Nicolas, J.-M., Loreaux, P., 2014. MIMOSA: an automatic change detection method for SAR time series. IEEE Trans. Geosci. Remote Sens.

Ray, D.K., Foley, J.A., 2013. Increasing global crop harvest frequency: recent trends and future directions. Environ. Res. Lett. 8, 44041–44050.

Sakamoto, T., Van Nguyen, N., Ohno, H., Ishitsuka, N., Yokozawa, M., 2006. Spatiotemporal distribution of rice phenology and cropping systems in the Mekong Delta with special reference to the seasonal water flow of the Mekong and Bassac rivers. Remote Sens. Environ. 100, 1–16.

Sakamoto, T., Van Phung, C., Kotera, A., Nguyen, K.D., Yokozawa, M., 2009. Analysis of rapid expansion of inland aquaculture and triple rice-cropping areas in a coastal area of the Vietnamese Mekong Delta using MODIS time-series imagery. Landscape Urban Plann. 92, 34–46.

Setiawan, Y., Rustiadi, E., Yoshino, K., Effendi, H., 2014a. Assessing the seasonal dynamics of the Java's Paddy field Using MODIS satellite images. ISPRS Int. J. Geo-Inf. 3, 110–129.

Setiawan, Y., Yoshino, K., Prasetyo, L.B., 2014b. Characterizing the dynamics change of vegetation cover on tropical forestlands using 250 m multi-temporal MODIS EVI. Int. J. Appl. Earth Observ. Geoinf. 26, 132–144.

Siebert, S., Ewert, F., 2012. Spatio-temporal patterns of phenological development in Germany in relation to temperature and day length. Agric. For. Meteorol. 152, 44–57.

Stueve, K.M., Housman, I.W., Zimmerman, P.L., Nelson, M.D., Webb, J.B., Perry, C.H., Chastain, R.A., Gormanson, D.D., Huang, C., Healey, S.P., Cohen, W.B., 2011. Snow-covered Landsat time series stacks improve automated disturbance mapping accuracy in forested landscapes. Remote Sens. Environ. 115, 3203– 3219.

Terletzky, P., Ramsey, R.D., 2014. A semi-automated single day image differencing technique to identify animals in aerial imagery. PLoS One 9, e85239.

Thenkabail, P.S., Wu, Z., 2012. An automated cropland classification algorithm (ACCA) for Tajikistan by combining Landsat, MODIS, and secondary data. Remote Sens. 4, 2890–2918.

Torrence, C., Compo, G.P., 1998. A practical guide to wavelet analysis. Bull. Am. Meteorol. Soc. 79, 61–78.

Tseng, Y.-H., Wang, C.-K., Chu, H.-J., Hung, Y.-C., 2015. Waveform-based point cloud classification in land-cover identification. Int. J. Appl. Earth Observ. Geoinf. 34, 78–88.

Waldner, F., Canto, G.S., Defourny, P., 2015. Automated annual cropland mapping using knowledge-based temporal features. ISPRS J. Photogramm. Remote Sens. 110, 1–13.

Wardlow, B.D., Egbert, S.L., Kastens, J.H., 2007. Analysis of time-series MODIS 250 m vegetation index data for crop classification in the US Central Great Plains. Remote Sens. Environ. 108, 290–310.

Wu, Z., Thenkabail, P.S., Verdin, J.P., 2014. Automated Cropland Classification Algorithm (ACCA) for California using multi-sensor remote sensing. Photogramm. Eng. Remote Sens. 80, 81–90.

Yan, L., Roy, D.P., 2014. Automated crop field extraction from multi-temporal Web Enabled Landsat Data. Remote Sens. Environ. 144, 42–64.

Zhang, J., Pu, R., Loraamm, R.W., Yang, G., Wang, J., 2014. Comparison between wavelet spectral features and conventional spectral features in detecting yellow rust for winter wheat. Comput. Electron. Agric. 100, 79–87.

Zhang, M., Zhou, Q., Chen, Z., Liu, J., Zhou, Y., Cai, C., 2008. Crop discrimination in Northern China with double cropping systems using Fourier analysis of time-series MODIS data. Int. J. Appl. Earth Observ. Geoinf. 10, 476–485.